61. Qu X, Zou Z, Sun Q, Luby-Phelps K, Cheng P, Hogan RN *et al.* Autophagy gene-dependent clearance of apoptotic cells during embryonic development. *Cell* 2007; **128**: 931–946.
62. Bradbury DA, Simmons TD, Slater KJ, Crouch SP. Measurement of the ADP:ATP ratio in human leukaemic cell lines can be used as an indicator of cell viability, necrosis and apoptosis. *J Immunol Methods* 2000; **240**: 79–92.
63. Tasdemir E, Maiuri MC, Galluzzi L, Vitale I, Djavaheri-Mergny M, D'Amelio M *et al.* Regulation of autophagy by cytoplasmic p53. *Nat Cell Biol* 2008; **10**: 676–687.
64. Vitale I, Galluzzi L, Vivet S, Nanty L, Dessen P, Senovilla L *et al.* Inhibition of Chk1 kills tetraploid tumor cells through a p53-dependent pathway. *PLoS ONE* 2007; **2**: e1337.
65. Baize S, Leroy EM, Georges-Courbot MC, Capron M, Lansoud-Soukate J, Debre P *et al.* Defective humoral responses and extensive intravascular apoptosis are associated with fatal outcome in Ebola virus-infected patients. *Nat Med* 1999; **5**: 423–426.
66. Bonfoco E, Krainc D, Ankarcrona M, Nicotera P, Lipton SA. Apoptosis and necrosis: two distinct events induced, respectively, by mild and intense insults with N-methyl-D-aspartate or nitric oxide/superoxide in cortical cell cultures. *Proc Natl Acad Sci USA* 1995; **92**: 7162–7166.
67. Krysko DV, Vanden Berghe T, D'Herde K, Vandenabeele P. Apoptosis and necrosis: detection, discrimination and phagocytosis. *Methods* 2008; **44**: 205–221.
68. Krysko DV, Vanden Berghe T, Parthoens E, D'Herde K, Vandenabeele P. Methods for distinguishing apoptotic from necrotic cells and measuring their clearance. *Methods Enzymol* 2008; **442**: 307–341.
69. Belzacq-Casagrande AS, Martel C, Pertuiset C, Borgne-Sanchez A, Jacotot E, Brenner C. Pharmacological screening and enzymatic assays for apoptosis. *Front Biosci* 2009; **14**: 3550–3562.
70. Blattner JR, He L, Lemasters JJ. Screening assays for the mitochondrial permeability transition using a fluorescence multiwell plate reader. *Anal Biochem* 2001; **295**: 220–226.
71. Tao Y, Zhang P, Girdler F, Frascogna V, Castedo M, Bourhis J *et al.* Enhancement of radiation response in p53-deficient cancer cells by the Aurora-B kinase inhibitor AZD1152. *Oncogene* 2008; **27**: 3244–3255.
72. Wyllie AH. Glucocorticoid-induced thymocyte apoptosis is associated with endogenous endonuclease activation. *Nature* 1980; **284**: 555–556.
73. George TC, Basiji DA, Hall BE, Lynch DH, Ortyn WE, Perry DJ *et al.* Distinguishing modes of cell death using the ImageStream multispectral imaging flow cytometer. *Cytometry A* 2004; **59**: 237–245.
74. Pouliquen D, Bellot G, Guihard G, Fichet P, Meflah K, Vallette FM. Mitochondrial membrane permeabilization produced by PTP, Bax and apoptosis: a 1H-NMR relaxation study. *Cell Death Differ* 2006; **13**: 301–310.
75. Crouser ED, Gadd ME, Julian MW, Huff JE, Broekemeier KM, Robbins KA *et al.* Quantitation of cytochrome c release from rat liver mitochondria. *Anal Biochem* 2003; **317**: 67–75.
76. Patterson SD, Spahr CS, Daugas E, Susin SA, Irinopoulou T, Koehler C *et al.* Mass spectrometric identification of proteins released from mitochondria undergoing permeability transition. *Cell Death Differ* 2000; **7**: 137–144.
77. Obeid M, Tesniere A, Ghiringhelli F, Fimia GM, Apetoh L, Perfettini JL *et al.* Calreticulin exposure dictates the immunogenicity of cancer cell death. *Nat Med* 2007; **13**: 54–61.
78. Galluzzi L, Joza N, Tasdemir E, Maiuri MC, Hengartner M, Abrams JM *et al.* No death without life: vital functions of apoptotic effectors. *Cell Death Differ* 2008; **15**: 1113–1123.
79. Timmer JC, Salvesen GS. Caspase substrates. *Cell Death Differ* 2007; **14**: 66–72.
80. De Maria R, Zeuner A, Eramo A, Domenichelli C, Bonci D, Grignani F *et al.* Negative regulation of erythropoiesis by caspase-mediated cleavage of GATA-1. *Nature* 1999; **401**: 489–493.
81. Zermati Y, Garrido C, Amsellem S, Fishelson S, Bouscary D, Valensi F *et al.* Caspase activation is required for terminal erythroid differentiation. *J Exp Med* 2001; **193**: 247–254.
82. Janicke RU, Sohn D, Schulze-Osthoff K. The dark side of a tumor suppressor: anti-apoptotic p53. *Cell Death Differ* 2008; **15**: 959–976.

Biochemical and Biophysical Research Communications 378 (2009) 186–191

Contents lists available at ScienceDirect

Biochemical and Biophysical Research Communications

journal homepage: www.elsevier.com/locate/ybbrc

Adenovirus-mediated gene transfer of adiponectin reduces the severity of collagen-induced arthritis in mice

Kosuke Ebina [a,b], Kazuya Oshima [a], Morihiro Matsuda [b,c,d], Atsunori Fukuhara [b], Kazuhisa Maeda [b], Shinji Kihara [b], Jun Hashimoto [a], Takahiro Ochi [e], Nirmal K. Banda [f], Hideki Yoshikawa [a], Iichiro Shimomura [a,*]

[a] Departments of Orthopaedics and Metabolic Medicine, Graduate School of Medicine, Osaka University, 2-2 Yamadaoka, Suita, Osaka 565-0871, Japan
[b] Metabolic Medicine, Graduate School of Medicine, Osaka University, 2-2 Yamadaoka, Suita, Osaka 565-0871, Japan
[c] Division of Analysis for Pathophysiology, Institute of Clinical Research, National Hospital Organization Kure Medical Center, Kure, Hiroshima 737-0023, Japan
[d] Department of Internal Medicine, National Hospital Organization Kure Medical Center, Kure, Hiroshima 737-0023, Japan
[e] Osaka Police Hospital, 10-31 Kitayama-cho, Tennoji-ku, Osaka 543-0035, Japan
[f] Division of Rheumatology B115, University of Colorado at Denver and Health Sciences Center, M-20 3104, 1775 North Ursula St., Aurora, CO 80045, USA

ARTICLE INFO

Article history:
Received 24 October 2008
Available online 21 November 2008

Keywords:
Adiponectin
Collagen-induced arthritis
Complement
Disease severity
Inflammation
Mice
Rheumatoid arthritis

ABSTRACT

Adiponectin (APN) is a hormone released by adipose tissue with anti-inflammatory properties. The purpose of this study was to examine the therapeutic effects of systemic delivery of APN in murine arthritis model. Collagen-induced arthritis (CIA) was induced in male DBA1/J mice, and adenoviral vectors encoding human APN (Ad-APN) or beta-galactosidase (Ad-β-gal) as control were injected either before or during arthritis progression. Systemic APN delivery at both time points significantly decreased clinical disease activity scores of CIA. In addition, APN treatment before arthritis progression significantly decreased histological scores of inflammation and cartilage damage, bone erosion, and mRNA levels of pro-inflammatory cytokines in the joints, without altering serum anti-collagen antibodies levels. Immunohistochemical staining showed significant inhibition of complement C1q and C3 deposition in the joints of Ad-APN infected CIA mice. These results provide novel evidence that systemic APN delivery prevents inflammation and joint destruction in murine arthritis model.

Rheumatoid arthritis (RA) is an autoimmune disease characterized by chronic inflammation of joint synovial tissues, followed by cartilage destruction and bone erosion. Collagen-induced arthritis (CIA) is an established rodent model of autoimmune polyarthritis with many similarities to human RA, and the immunopathological process of CIA has been reported in details [1]. Briefly, injection of chicken type II collagen (CII) in complete Freund's adjuvant (CFA) results in proliferation and differentiation of T-cells into CD4+Th1-cells in the draining lymph nodes. These cells then promote the production of anti-collagen IgG by activated CII-specific B-cells. These antibodies enter the joint and bind to CII, forming an immunocomplex (IC), which activates the complement cascade. Complement enhances the permeability of the vascular endothelium, and facilitates infiltration of monocytes (macrophages) and neutrophils into the joint. In the joint space, macrophages produce tumor necrosis factor (TNF)-α and interleukin (IL)-1. TNF-α enhances vascular permeability and migration of inflammatory cells into the joint space, and IL-1 is the primary trigger of tissue destruction by infiltrating cells and resident synoviocytes.

Adiponectin (APN) is an adipocytokine that shares strong homologies with the complement factor C1q and TNF-α [2]. APN has anti-inflammatory effects, and suppresses TNF-α and IL-6 production by macrophages activated with lipopolysaccharide (LPS) through suppression of nuclear factor-kappa B (NF-κB) signaling [3]. Accumulating evidence suggests a novel link between APN and inflammatory joint diseases. For example, APN concentration in the synovial fluid correlates negatively with synovial fluid leukocyte count in patients with RA, suggesting that APN is an anti-inflammatory molecule in RA [4]. However, APN levels in synovial fluid and serum are elevated in patients with RA compared with healthy controls [4], and APN treatment induces IL-6 production by synovial fibroblasts from RA patients [5], suggesting that APN is a pro-inflammatory molecule in RA. Thus, the effects of APN in RA are controversial. In the present study, we investigated the effects of APN on CIA mice using APN-producing adenovirus.

Materials and methods

Materials. Enzyme-linked immunosorbent assay (ELISA) for murine APN (including all isoforms) was purchased from Otsuka Pharmaceutical (Tokyo, Japan). Anti-APN polyclonal antibody used

* Corresponding author. Fax: +81 6 6879 3739.
E-mail address: ichi@imed2.med.osaka-u.ac.jp (I. Shimomura).

0006-291X/$ - see front matter © 2008 Elsevier Inc. All rights reserved.
doi:10.1016/j.bbrc.2008.11.005

for Western blotting was described previously [6]. Tartrate-resistant acid phosphatase (TRAP) staining kit was purchased from Cell Garage (Tokyo, Japan).

Induction and assessment of CIA. To induce CIA, we injected intradermally 100 μl of an emulsion containing 200 μg of chicken CII (Sigma, St. Louis, MO) and 200 μg of *Mycobacterium tuberculosis* in CFA (Chondrex, Redmond, WA) at the base of the tail of 6-week-old male DBA/1J mice (CLEA Japan, Tokyo), twice with a 21-day gap, as described previously [7]. Clinical severity of arthritis was assessed as described previously [8]. Each limb was scored, yielding a maximum possible score of 16 per mouse. Serum was collected from the tail vein at each time point.

APN adenovirus and systemic delivery in vivo. Adenovirus producing the full-length mouse APN was prepared as described previously [9]. Then, 200 μl of 2×10^8 plaque-forming units of adiponectin-producing adenovirus (Ad-APN) or control β-galactosidase-expressing adenovirus (Ad-β-gal) were injected into the jugular vein, on 19 (before arthritis progression) or 27 (during arthritis progression) days after initial injection of CII.

Determination of IgG, IgG2a, and IgG1 titers against CII and serum complement C1q and C3 levels. The total IgG anti-collagen antibody titers against chicken CII were determined through ELISA kit (Chondrex). IgG1 and IgG2a anti-collagen antibody titers against chicken CII were determined as described previously, and expressed in optical density (OD) value [10]. Serum C1q and C3 levels were determined by ELISA as described previously [11].

Histological analysis. On day 35 after initial injection of CII, joints were harvested and fixed in phosphate-buffered 4% paraformaldehyde, decalcified in 14% ethylenediaminetetraacetic acid (EDTA), and embedded in paraffin. Joint sections were stained with Safranin O and hematoxylin/eosin, and then histologically scored for inflammation, cartilage damage, and pannus formation as described previously [12]. Immunostaining for mouse IgG, C1q, C3, neutrophils, CXC chemokine ligand (CXCL)12, and APN was performed on paraffin-embedded samples with goat anti-mouse IgG (Cappel), rat anti-mouse C1q (Hycult Biotechnology b.v., Uden, Netherlands), rat anti-mouse C3 (Hycult Biotechnology), rat-anti-mouse neutrophils, (Serotec, Oxford, UK), monoclonal antihuman/mouse CXCL12 antibody (R&D Systems Inc., Minneapolis, MN), and rabbit-anti-mouse APN (Otsuka Pharmaceutical), respectively. The other steps were performed according to the instructions provided on the labeling of Vectastain Elite ABC system (Vector Laboratories, Burlingame, CA). Scoring for IgG, C1q and C3 staining on the cartilage, and CXCL12 staining on the synovium was performed as described previously [13]. The average number of infiltrating neutrophils in the synovium was determined using a modified version of the published method [14].

Quantitative real-time PCR of joint samples. Total RNA was extracted by pulverizing the frozen individual fore paws with an RNA STAT-60 kit. The first-strand cDNA was synthesized using ThermoScript RT-PCR System (Invitrogen, San Diego, CA). Real-time polymerase chain reaction (PCR) was performed on a Light Cycler using the Fast Start DNA Master SYBR Green I (Roche Diagnostics, Indianapolis, IN). The sequences of primers were designed based on a previous report [13], and other primers are listed in Supplementary Table 1.

Lymph node cell proliferation assay. In vitro proliferation of draining lymph node (DLN) cells was examined by Cell Proliferation ELISA Bromodeoxyuridine (BrdU) kit (Roche) using a modified version of the published method [10].

Cytokine production by cultured splenocytes. Spleens were removed and cell suspensions (2×10^6 cells/well) were distributed to flat bottom 96-well plates. Spleen cells were cultured without or with either 50 μg/ml heat-denatured chicken CII (Sigma–Aldrich) or 5 μg/ml LPS from *Escherichia coli* (Sigma–Aldrich). After 48-h incubation, the supernatants were collected, and TNF-α and IL-1β levels were measured using ELISA kit (Quantikine Mouse ELISA kit, R&D Systems Inc.).

Skeletal morphology. Three-dimensional microcomputed tomography (3D-μCT) scan for ankle joints was undertaken and the trabecular bone area (percentage of bone volume [BV] per tissue volume [TV]) of distal tibia was measured using a composite X-ray analysis system (Shimadzu, SMX-100CT-SV, Kyoto, Japan).

Statistical analysis and ethical considerations. Data were expressed as means ± standard error of the mean. Differences between groups were examined for statistical significance using Chi-square test, Student's *t* test, or analysis of variance with Fisher's protected least significant difference test. A *P* value less than 0.05 denoted the presence of a statistically significant difference. The experimental protocol was approved by the Ethics Review Committee for Animal Experimentation of Osaka University School of Medicine.

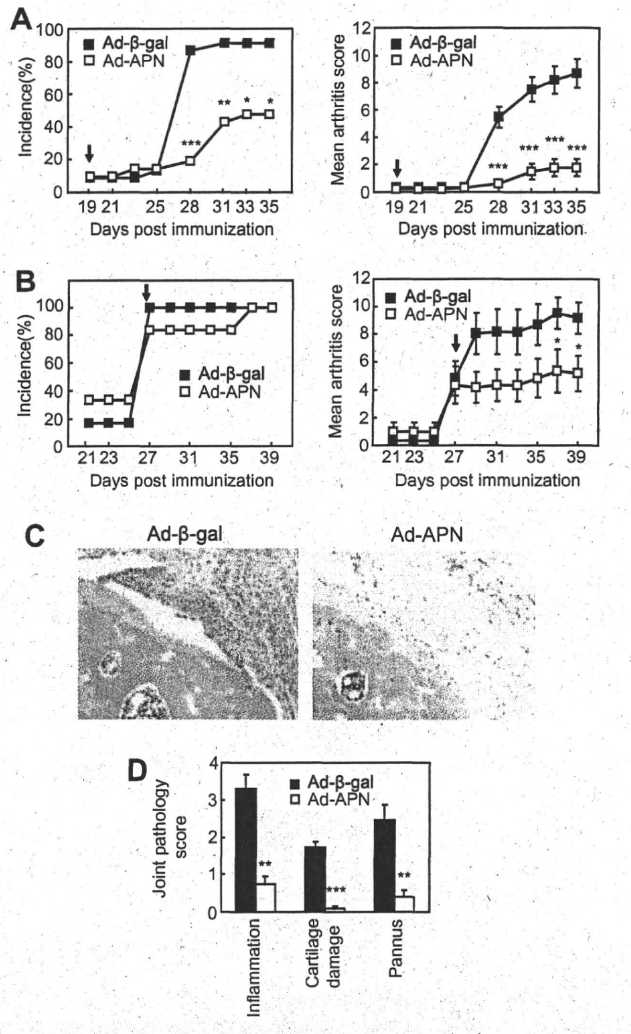

Fig. 1. Systemic delivery of APN in collagen-induced arthritis (CIA) mouse model and histological analysis of the joints. (A) On day 19, before arthritis progression, mice were injected with adenoviral vector directing the expression of either *lacZ* gene (Ad-β-gal) or APN (Ad-APN) intravenously ($n = 23$ Ad-β-gal-infected mice, $n = 21$ Ad-APN-infected mice). (B) On day 27, during arthritis progression, mice were injected with the same adenovirus ($n = 6$ mice in each group). (C) Histological features of representative hematoxylin and eosin-stained sections of the ankle joints (original magnification 200×), and (D) mean pathological scores of the joints of adenovirus-infected CIA mice ($n = 36$ joints in each group). $^{*}P < 0.05$, $^{**}P < 0.01$, $^{***}P < 0.001$, versus Ad-β-gal-infected CIA mice.

Results

Ad-APN suppresses progression of arthritis in CIA model

First, we tried two protocols to evaluate the effect of Ad-APN on CIA. When the virus was injected on day 19 (Fig. 1A), the incidence and disease activity on day 35 were significantly suppressed by Ad-APN treatment compared with Ad-β-gal (arthritis score: Ad-APN-infected mice: 1.76 ± 0.63, Ad-β-gal-infected mice: 8.68 ± 1.06; $P < 0.001$). In addition, when the virus was injected on day 27 (Fig. 1B), disease activity was significantly suppressed on day 39 by Ad-APN treatment compared with Ad-β-gal (arthritis score: Ad-APN-infected mice: 5.17 ± 1.25, Ad-β-gal-infected mice: 9.17 ± 1.15; $P < 0.05$). For the rest of this study, we used the former protocol (Fig. 1A). Histological analysis of the ankle joint showed typical features of active arthritis in Ad-β-gal-infected CIA mice, including infiltration of inflammatory cells into the synovium, cartilage damage, and pannus formation. These changes were significantly less pronounced in Ad-APN-infected CIA mice (Fig. 1C and D).

Ad-APN increases APN protein in serum and bone marrow, and does not alter serum anti-collagen antibodies or complement levels

In the experiments described in Fig. 1A, injection of Ad-APN resulted in about 5-fold increase on day 21 and about 30-fold increase on day 35 in serum APN levels (Fig. 2A). The high serum APN protein levels in Ad-APN-infected CIA mice were mainly composed of high- and middle-molecular weight forms of APN (Fig. 2B). Moreover, Ad-APN substantially increased APN protein content in knee joints compared with Ad-β-gal (Fig. 2C). Immunohistochemical staining of knee joints with anti-APN antibody indicated accumulation of APN in the bone marrow but not on the cartilage surface in Ad-APN-infected CIA mice (Fig. 2D). Under such conditions, anti-CII IgG, IgG2a, and IgG1 titers, serum C1q and C3 levels were not different between Ad-APN- and Ad-β-gal-infected CIA mice (Fig. 2E and F).

Treatment of CIA mice with Ad-APN suppresses local deposition of C1q and C3, infiltration of neutrophil, and changes in mRNAs of pro-inflammatory genes

Next, we examined the accumulation of IgG, C1q, and C3 on the cartilage of wrist, knee, and ankle joints by immunohistochemical staining (Fig. 3A and B). Under the conditions with minimum background staining, IgG deposition on the cartilage was observed in both adenovirus-infected CIA mice. On the other hand, C1q and C3 deposits on the cartilage were significantly suppressed by Ad-APN treatment compared with Ad-β-gal. Furthermore, neutrophil infiltration and synovium deposition of CXCL12, a chemokine that promotes leukocyte migration, were also significantly decreased in Ad-APN-infected CIA mice (Fig. 3A and B). To assess the inflammatory status, mRNA levels of pro-inflammatory genes, complement factors, and F4/80 (a marker of monocyte/macrophage linage) were measured in isolated forepaws. The expression levels of IL-1β, IL-6, COX-2 IFN-γ, TNF-α, C1q, C3, and F4/80 were all significantly decreased by Ad-APN treatment (Fig. 3C).

Effects of Ad-APN on immunocyte activities in lymph nodes and spleen, and bone erosion of CIA mice

Next, activities of immunocytes were measured. DLN cells from Ad-APN-infected CIA mice showed marginally inhibited proliferation activities (Fig. 4A). Splenocytes from Ad-APN-infected CIA

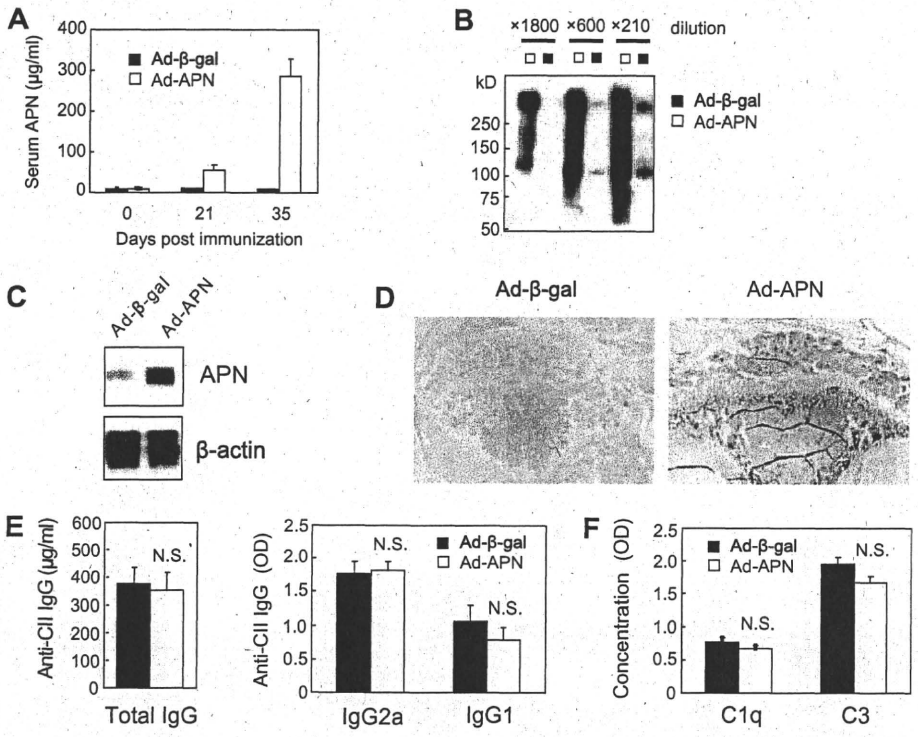

Fig. 2. High APN levels in serum and joints do not alter serum levels of anti-CII antibody, complement C1q, or C3 in CIA mice. (A) Serum APN concentrations at each time point were determined by ELISA ($n = 6$ in each group). Representative serum samples (B) and protein lysates prepared from knee joints (C) of adenovirus-infected CIA mice on day 35 were subjected sodium dodecyl sulfate-polyacrylamide gel electrophoresis without reducing reagent, and analyzed by western blot using anti-APN antibody. (D) Representative sections of proximal tibia immunostained with APN (original magnification 40×). Serum samples were obtained on day 35, and anti-CII specific IgG, IgG2a, and IgG1 levels (E), and complement C1q and C3 levels (F) were measured by ELISA ($n = 6$ in each group). NS = not significant.

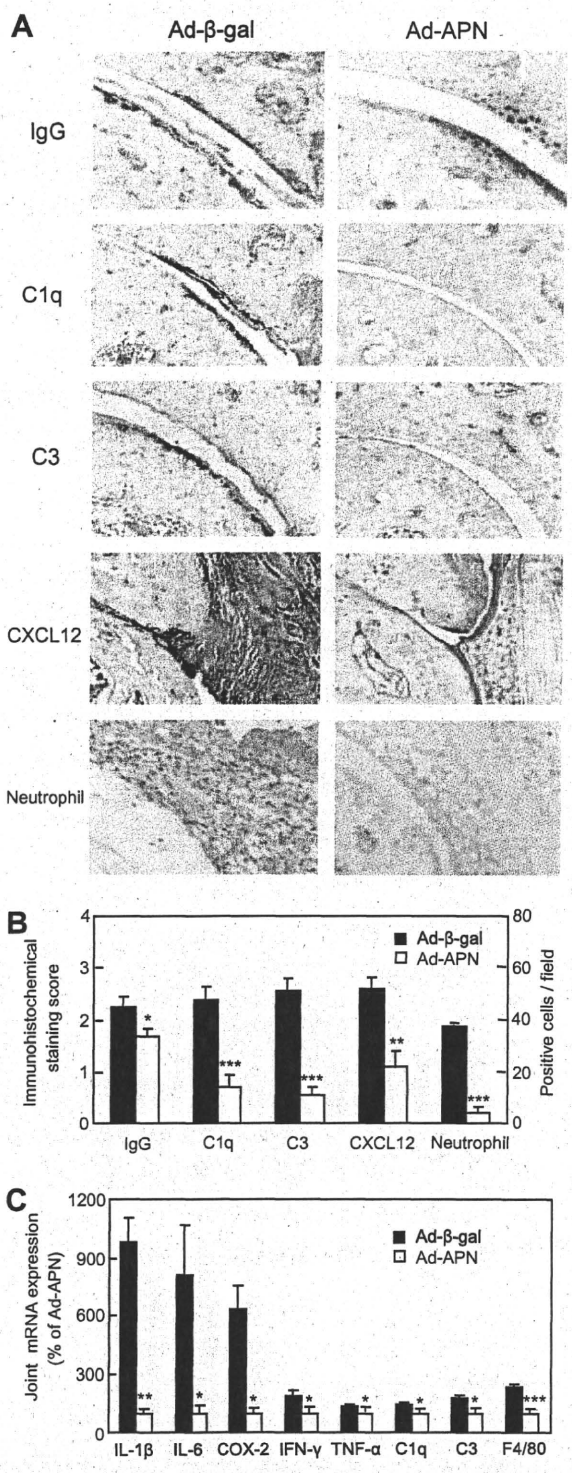

Fig. 3. Ad-APN inhibits complement deposition/expression and pro-inflammatory cytokine/enzyme expression in CIA mice. (A) Representative sections immunostained for IgG, C1q, C3, CXCL12, and neutrophil on the cartilage surface and synovium of the ankle joints of adenovirus-infected CIA mice (original magnification 200×). (B) Scoring of immunostained joint sections from adenovirus-infected CIA mice ($n = 16$ joints in each group). (C) mRNA expression levels in forepaws of adenovirus-infected CIA mice. ($n = 6$ joints in each group). Values are normalized to the level of 36B4 mRNA. $^{*}P < 0.05$, $^{**}P < 0.01$, $^{***}P < 0.001$, versus Ad-β-gal-infected CIA mice.

mice produced less IL-1β in all conditions, and less TNF-α in response to LPS *in vitro* (Fig. 4B). Finally, analysis of bone erosion of the distal tibia using μCT revealed that trabecular bone volume were significantly decreased in Ad-β-gal-infected CIA mice compared to those in Ad-APN-infected CIA mice (Fig. 4C). In addition, the number of TRAP-positive cells was significantly decreased in ankle joints of Ad-APN-infected CIA mice (Fig. 4D).

Discussion

In the present study, we demonstrated for the first time that Ad-APN significantly improved joint inflammation and bone erosion in CIA mice. There were no significant differences in anti-CII IgG, C1q, and C3 levels between Ad-APN and Ad-β-gal infected CIA mice (Fig. 2E and F), indicating that Ad-APN has little effect on humoral immunity. On the other hand, C1q and C3 deposition were markedly suppressed on the cartilage surface of Ad-APN-infected CIA mice (Fig. 3A and B). Therefore, we investigated the direct effect of APN on complement activation. APN has a substantial sequence similarity to C1q, and also binds to C1q receptor [15]. In addition, we confirmed the binding between human recombinant APN from mammalian cells and human C1q *in vitro* as reported previously [16]. However, in our preliminary experiments, this recombinant APN did not alter C1q binding to adherent CII-IC [11], CII-IC-induced mouse serum C3 activation (mainly involves classical pathway) [11], or zymosan-induced mouse serum C3 activation (mainly involves alternative pathway) [10] *in vitro* (data not shown). To elucidate the direct effect of APN on the complement activation, further *in vivo* and *in vitro* analyses are required.

We showed marked suppression of C1q and C3 deposition, accompanied by significant downregulation of C1q, C3, and F4/80 mRNAs in the Ad-APN-infected CIA joints (Fig. 3). A previous report demonstrated that APN inhibited the expression of endothelial adhesion molecules induced by TNF-α, and consequent transendothelial migration of monocytes [17]. In addition, TNF-α-induced vascular permeability is required for the migration of inflammatory cells into the joint and development of inflammatory process in mouse arthritis models [1], and APN was reported to inhibit TNF-α-induced hyperpermeability in endothelial cells [18]. Our group demonstrated that APN was protective against murine colitis through inhibition of macrophages infiltration and release of pro-inflammatory cytokines [19]. Considering that C1q is mainly produced by monocyte/macrophage linage [20], and C3 is produced by liver and inflamed synoviocytes [21], reduced accumulation of F4/80 positive cells and consequent C3 production by inflamed synovium should result in suppression of complement deposition and pro-inflammatory cytokine production in the CIA joints.

We also observed that Ad-APN suppressed synovial deposition of CXCL12. CXCL12 is a chemokine anchored to heparan sulfate (HS) proteoglycans on endothelial cells of RA synovium [22], and acts as a critical chemoattractant in the pathogenesis of CIA [23]. APN inhibits the binding of CXCL12 to HS, and alters the distribution of CXCL12 at the site of inflammation [24]. Taken together, Ad-APN may improve joint inflammation through decreased CXCL12 deposition in CIA synovium.

Previous studies showed that the cellular immunity, represented by the activity of immunocytes of lymph nodes or spleen, is causally associated with the disease activity in CIA mice [25]. In this study, Ad-APN marginally reduced DLN cells proliferation (Fig. 4A), and significantly suppressed IL-1β production and TNF-α production from splenocytes (Fig. 4B). These results indicate that Ad-APN could suppress disease activity of CIA partially through inhibition of cellular immunity.

In this study, Ad-APN reduced the number of TRAP-positive cells and resulted in amelioration of bone erosion in the joints of CIA mice (Fig. 4C and D). Previously, we and others reported that

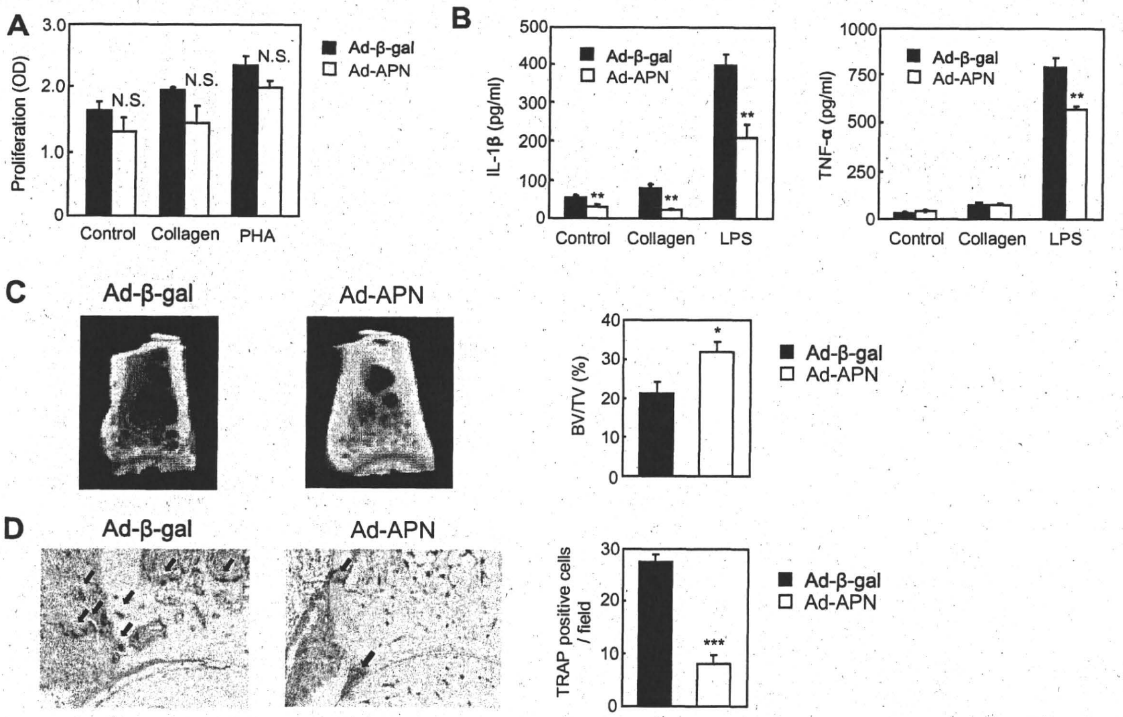

Fig. 4. Effects of Ad-APN on DLN cell proliferation and pro-inflammatory cytokine production from splenocytes, and bone erosion in CIA. All samples were obtained on day 35. (A) Proliferative response of DLN cells obtained from adenovirus-infected CIA mice. Isolated cells from lymph nodes were cultured for 72 h without (control) or with either 50 μg/ml heat-denatured chicken CII or 5 μg/ml phytohemagglutinin (PHA). (B) Production of pro-inflammatory cytokine by splenocytes from adenovirus-infected CIA mice. IL-1β and TNF-α levels were measured in supernatants of splenocytes by specific ELISA. (C) Three-dimensional μCT scan of the distal tibia of adenovirus-infected CIA mice. Trabecular bone volume is expressed as percentage of total tissue volume (BV/TV [%]) ($n = 4$ joints in each group). (D) Reduced number of osteoclasts in Ad-APN-infected CIA mice joints. Sections of ankle joints stained with TRAP (original magnification 100×). The number of TRAP-positive cells was counted in 5 randomly selected fields ($n = 8$ joints in each group). NS = not significant, $^{*}P < 0.05$, $^{**}P < 0.01$, $^{***}P < 0.001$, versus Ad-β-gal-infected CIA mice.

APN inhibits osteoclasts differentiation in RAW264 cells [26] and mouse bone marrow macrophages [9]. Collectively, besides anti-inflammatory effects in the joints, Ad-APN might directly inhibits bone erosion of CIA mice by inhibiting osteoclasts differentiation.

The present study demonstrates for the first time that systemic APN delivery provides protection against the development of inflammatory arthritis in a murine model, through several anti-inflammatory mechanisms. The results provide new insights on the role of APN in inflammatory arthritis and new strategies for the treatment.

Acknowledgments

We are grateful to Dr. T. Maeda for great help with the experiments. We also thank M. Shinkawa and F. Katsube for the excellent support in tissue processing for histological analysis. This work was supported by grants from the Ministry of Health, Labour, and Welfare of Japan.

Appendix A. Supplementary data

Supplementary data associated with this article can be found, in the online version, at doi:10.1016/j.bbrc.2008.11.005.

References

[1] J.A. Luross, N.A. Williams, The genetic and immunopathological processes underlying collagen-induced arthritis, Immunology 103 (2001) 407–416.
[2] P.E. Scherer, S. Williams, M. Fogliano, G. Baldini, H.F. Lodish, A novel serum protein similar to C1q, produced exclusively in adipocytes, J. Biol. Chem. 270 (1995) 26746–26749.
[3] M.C. Wulster-Radcliffe, K.M. Ajuwon, J. Wang, J.A. Christian, M.E. Spurlock, Adiponectin differentially regulates cytokines in porcine macrophages, Biochem. Biophys. Res. Commun. 316 (2004) 924–929.
[4] L. Senolt, K. Pavelka, D. Housa, M. Haluzik, Increased adiponectin is negatively linked to the local inflammatory process in patients with rheumatoid arthritis, Cytokine 35 (2006) 247–252.
[5] C.H. Tang, Y.C. Chiu, T.W. Tan, R.S. Yang, W.M. Fu, Adiponectin enhances IL-6 production in human synovial fibroblast via an AdipoR1 receptor, AMPK, p38, and NF-kappa B pathway, J. Immunol. 179 (2007) 5483–5492.
[6] N. Maeda, M. Takahashi, T. Funahashi, S. Kihara, H. Nishizawa, K. Kishida, H. Nagaretani, M. Matsuda, R. Komuro, N. Ouchi, H. Kuriyama, K. Hotta, T. Nakamura, I. Shimomura, Y. Matsuzawa, PPARgamma ligands increase expression and plasma concentrations of adiponectin, an adipose-derived protein, Diabetes 50 (2001) 2094–2099.
[7] S. Nakae, A. Nambu, K. Sudo, Y. Iwakura, Suppression of immune induction of collagen-induced arthritis in IL-17-deficient mice, J. Immunol. 171 (2003) 6173–6177.
[8] E. Gonzalez-Rey, A. Chorny, N. Varela, F. O'Valle, M. Delgado, Therapeutic effect of urocortin on collagen-induced arthritis by down-regulation of inflammatory and Th1 responses and induction of regulatory T cells, Arthritis Rheum. 56 (2007) 531–543.
[9] K. Oshima, A. Nampei, M. Matsuda, M. Iwaki, A. Fukuhara, J. Hashimoto, H. Yoshikawa, I. Shimomura, Adiponectin increases bone mass by suppressing osteoclast and activating osteoblast, Biochem. Biophys. Res. Commun. 331 (2005) 520–526.
[10] N.K. Banda, D. Kraus, A. Vondracek, L.H. Huynh, A. Bendele, V.M. Holers, W.P. Arend, Mechanisms of effects of complement inhibition in murine collagen-induced arthritis, Arthritis Rheum. 46 (2002) 3065–3075.
[11] N.K. Banda, K. Takahashi, A.K. Wood, V.M. Holers, W.P. Arend, Pathogenic complement activation in collagen antibody-induced arthritis in mice requires amplification by the alternative pathway, J. Immunol. 179 (2007) 4101–4109.
[12] A. Bendele, T. McAbee, G. Sennello, J. Frazier, E. Chlipala, D. McCabe, Efficacy of sustained blood levels of interleukin-1 receptor antagonist in animal models of arthritis: comparison of efficacy in animal models with human clinical data, Arthritis Rheum. 42 (1999) 498–506.
[13] N.K. Banda, J.M. Thurman, D. Kraus, A. Wood, M.C. Carroll, W.P. Arend, V.M. Holers, Alternative complement pathway activation is essential for inflammation and joint destruction in the passive transfer model of collagen-induced arthritis, J. Immunol. 177 (2006) 1904–1912.

[14] Z. Liu, X. Xu, H.C. Hsu, A. Tousson, P.A. Yang, Q. Wu, C. Liu, S. Yu, H.G. Zhang, J.D. Mountz, CII-DC-AdTRAIL cell gene therapy inhibits infiltration of CII-reactive T cells and CII-induced arthritis, J. Clin. Invest. 112 (2003) 1332–1341.
[15] T. Yokota, K. Oritani, I. Takahashi, J. Ishikawa, A. Matsuyama, N. Ouchi, S. Kihara, T. Funahashi, A.J. Tenner, Y. Tomiyama, Y. Matsuzawa, Adiponectin, a new member of the family of soluble defense collagens, negatively regulates the growth of myelomonocytic progenitors and the functions of macrophages, Blood 96 (2000) 1723–1732.
[16] P.W. Peake, Y. Shen, A. Walther, J.A. Charlesworth, Adiponectin binds C1q and activates the classical pathway of complement, Biochem. Biophys. Res. Commun. 367 (2008) 560–565.
[17] N. Ouchi, S. Kihara, Y. Arita, K. Maeda, H. Kuriyama, Y. Okamoto, K. Hotta, M. Nishida, M. Takahashi, T. Nakamura, S. Yamashita, T. Funahashi, Y. Matsuzawa, Novel modulator for endothelial adhesion molecules: adipocyte-derived plasma protein adiponectin, Circulation 100 (1999) 2473–2476.
[18] S.Q. Xu, K. Mahadev, X. Wu, L. Fuchsel, S. Donnelly, R.G. Scalia, B.J. Goldstein, Adiponectin protects against angiotensin ii or tumor necrosis factor {alpha}-induced endothelial cell monolayer hyperpermeability. Role of cAMP/PKA signaling, Arterioscler Thromb. Vasc. Biol. (2008).
[19] T. Nishihara, M. Matsuda, H. Araki, K. Oshima, S. Kihara, T. Funahashi, I. Shimomura, Effect of adiponectin on murine colitis induced by dextran sulfate sodium, Gastroenterology 131 (2006) 853–861.
[20] Y. Takemura, N. Ouchi, R. Shibata, T. Aprahamian, M.T. Kirber, R.S. Summer, S. Kihara, K. Walsh, Adiponectin modulates inflammatory reactions via calreticulin receptor-dependent clearance of early apoptotic bodies, J. Clin. Invest. 117 (2007) 375–386.
[21] P.A. Monach, A. Verschoor, J.P. Jacobs, M.C. Carroll, A.J. Wagers, C. Benoist, D. Mathis, Circulating C3 is necessary and sufficient for induction of autoantibody-mediated arthritis in a mouse model, Arthritis Rheum. 56 (2007) 2968–2974.
[22] J.L. Pablos, B. Santiago, M. Galindo, C. Torres, M.T. Brehmer, F.J. Blanco, F.J. Garcia-Lazaro, Synoviocyte-derived CXCL12 is displayed on endothelium and induces angiogenesis in rheumatoid arthritis, J. Immunol. 170 (2003) 2147–2152.
[23] B. De Klerck, L. Geboes, S. Hatse, H. Kelchtermans, Y. Meyvis, K. Vermeire, G. Bridger, A. Billiau, D. Schols, P. Matthys, Pro-inflammatory properties of stromal cell-derived factor-1 (CXCL12) in collagen-induced arthritis, Arthritis Res. Ther. 7 (2005) R1208–1220.
[24] H. Masaie, K. Oritani, T. Yokota, I. Takahashi, T. Shirogane, H. Ujiie, M. Ichii, N. Saitoh, T. Maeda, R. Tanigawa, K. Oka, Y. Hoshida, Y. Tomiyama, Y. Kanakura, Adiponectin binds to chemokines via the globular head and modulates interactions between chemokines and heparan sulfates, Exp. Hematol. 35 (2007) 947–956.
[25] N.K. Banda, A. Vondracek, D. Kraus, C.A. Dinarello, S.H. Kim, A. Bendele, G. Senaldi, W.P. Arend, Mechanisms of inhibition of collagen-induced arthritis by murine IL-18 binding protein, J. Immunol. 170 (2003) 2100–2105.
[26] N. Yamaguchi, T. Kukita, Y.J. Li, N. Kamio, S. Fukumoto, K. Nonaka, Y. Ninomiya, S. Hanazawa, Y. Yamashita, Adiponectin inhibits induction of TNF-alpha/RANKL-stimulated NFATc1 via the AMPK signaling, FEBS Lett. 582 (2008) 451–456.

Clin Rheumatol (2009) 28:445–451
DOI 10.1007/s10067-008-1074-y

ORIGINAL ARTICLE

Serum adiponectin concentrations correlate with severity of rheumatoid arthritis evaluated by extent of joint destruction

Kosuke Ebina · Atsunori Fukuhara · Wataru Ando · Makoto Hirao · Tadashi Koga · Kazuya Oshima · Morihiro Matsuda · Kazuhisa Maeda · Tadashi Nakamura · Takahiro Ochi · Iichiro Shimomura · Hideki Yoshikawa · Jun Hashimoto

Received: 12 October 2008 / Revised: 30 November 2008 / Accepted: 3 December 2008 / Published online: 16 December 2008

Abstract Adiponectin is a hormone released by adipose tissue with antidiabetic, antiatherogenic, and anti-inflammatory properties. The present observational study focused on the relation between serum adiponectin level and the disease severity of established rheumatoid arthritis (RA). Ninety patients with more than 5-year diagnosis of RA and 42 age- and BMI-matched control were enrolled. The severity of RA was evaluated according to the number of destructed joints of overall 68 joints on plain radiographs (37 patients had mild RA and 53 had severe RA). Serum adiponectin level was significantly higher in the severe RA group (17.7±6.7 μg/ml) than in the control (9.1±3.8 μg/ml) and mild RA groups (13.9±6.5 μg/ml) (control vs. mild RA group, $P<0.001$; mild RA vs. severe RA group, $P<0.01$). These results suggest that increased number of joint destruction is associated with hyperadiponectinemia in established RA patients.

Keywords Adiponectin · Disease severity · Number of joint destruction · Rheumatoid arthritis

Introduction

Adiponectin is a hormone released by adipose tissue and has various biological properties, such as antidiabetic [1], antiatherogenic [2], and anti-inflammatory effects [3]. Part

K. Ebina · W. Ando · M. Hirao · K. Oshima · H. Yoshikawa · J. Hashimoto (✉)
Department of Orthopaedics, Graduate School of Medicine, Osaka University,
2-2 Yamadaoka,
Suita, Osaka 565-0871, Japan
e-mail: junha@ort.med.osaka-u.ac.jp

K. Ebina · A. Fukuhara · M. Matsuda · K. Maeda · T. Nakamura · I. Shimomura
Department of Metabolic Medicine, Graduate School of Medicine, Osaka University,
2-2 Yamadaoka,
Suita, Osaka 565-0871, Japan

T. Koga
Biometrics Department,
Shin Nippon Biomedical Laboratories, Ltd,
2438 Miyanoura,
Kagoshima, Kagoshima 891-1394, Japan

M. Matsuda
Division of Analysis for Pathophysiology,
Institute of Clinical Research,
National Hospital Organization Kure Medical Center,
Kure, Hiroshima 737-0023, Japan

M. Matsuda
Department of Internal Medicine,
National Hospital Organization Kure Medical Center,
Kure, Hiroshima 737-0023, Japan

T. Ochi
Osaka Police Hospital,
10-31 Kitayama-cho, Tennoji-ku,
Osaka 543-0035, Japan

of these effects is mediated by suppressing the production of tumor necrosis factor (TNF)-α and interleukin (IL)-6 by activated macrophage [3]. In addition, it has been reported that adiponectin stimulates the proliferation and differentiation of human osteoblasts [4] and suppresses the differentiation of osteoclasts [5], suggesting that adiponectin may play a role in rheumatoid arthritis (RA).

A recent clinical study showed that serum adiponectin concentrations are higher in RA patients than in healthy control [6, 7]. In addition, adiponectin induces the production of pro-inflammatory IL-6 from RA synovial fibroblasts in vitro [8], suggesting that adiponectin is a potent driving force of arthritis. On the other hand, another report demonstrated that adiponectin concentrations correlated negatively with the number of leukocytes in the synovial fluid of RA patients [7], indicating that adiponectin is a counterpart of the local inflammatory process. Thus, the role of adiponectin in RA is controversial. In a step to define the role of adiponectin in RA, the present study was designed to investigate the correlation between serum adiponectin level and RA disease severity.

Materials and methods

Patients

We have previously reported that serum adiponectin level is significantly higher in females than in males and negatively correlates with body mass index (BMI) [9]. In addition, previous reports have demonstrated that most of the progression of joint damage in RA occurs during the first years of the disease and decreases thereafter [10, 11]. Therefore, to investigate the correlation between serum adiponectin level and disease severity and joint destruction in established RA, 90 female patients with more than 5-year history of RA were enrolled in this study. RA was diagnosed based on the 1987 revised American College of Rheumatology (ACR) criteria [12]. The first assessment was carried out from September to November, 2005, and 18 patients were enrolled in the second assessment from March to April, 2008, about 2.5 years after the first assessment. Sixty-five patients (72.2%) were treated with oral prednisolone and 48 patients (53.3%) with methotrexate. All patients were followed-up at Osaka University Hospital.

For non-RA controls, 42 age- and BMI-matched women who underwent health examination at the institutions that participated in the Japanese Visceral Fat Syndrome (J-VFS) Study Committee of the Ministry of Health and Welfare of Japan and subjects who visited Osaka University Hospital for health check were enrolled in the present study [13]. Patients treated with antihypertensive, antidiabetic, or antihyperlipidemic regimen or patients who met the definition of each disease indicated in the relevant guidelines were defined as having hypertension, diabetes, and hyperlipidemia, respectively. Patients treated with drugs influencing serum adiponectin levels, such as anti-TNF-α [14, 15], insulin [16], thiazolidinediones [17], telmisartan [18], glimepiride [19], and all other biologics were excluded in this study. The study was approved by the Ethical Committee of Osaka University School of Medicine and written informed consent was obtained from each patient.

Assessment of disease severity and disease activity

The severity of RA was evaluated by the number of joints with erosions among 68 joints of whole body using plain radiographs, as described previously [20]. Joint erosion was defined as changes equal to or more severe than stage II according to the criteria of Steinbocker et al. [21]. Patients were classified according to disease severity as described previously [22]. Briefly, the least erosive subset (LES) group exhibited erosions in less than 20 joints and erosive articular changes limited to the small peripheral joints of hands or feet. The more erosive subset (MES) group had erosions in more than 21 joints and erosive articular changes in large axial joints. The most erosive subset with mutilating disease (MUD) group, that had erosions in more than 46 joints, and almost all joints were extensively damaged in the early period of RA. In this study, we categorized LES patients as the "mild RA group" (n=37), and MES/MUD patients as the "severe RA group" (n=53). Disease activity score including a 28 joint count/CRP (DAS28-CRP) was evaluated as described previously [23].

Measurement of serum adiponectin concentrations

Total serum adiponectin level (including all isoforms) was measured with an enzyme-linked immunosorbent assay (ELISA) kit (Otsuka Pharmaceutical, Tokyo, Japan), as reported previously [13].

Statistical analysis

Data are expressed as mean ± standard deviation (SD). Differences in variables between the mild and severe RA groups were assessed by the Mann–Whitney U test and the chi-square test. Changes in serum adiponectin levels between the first and second assessment was examined by the Wilcoxon's signed rank test. The influence of serum adiponectin level on other variables was investigated by calculating Spearman's correlation coefficients. The correlation between BMI and disease severity was investigated by logistic regression analysis. Conditional multivariate logistic regression models were constructed and odds ratios (ORs) and 95% confidence intervals (95% CI) were cal-

culated to investigate the association of serum adiponectin level on disease severity, with adjustment for BMI. To investigate the cutoff value for serum adiponectin, a value yielding 80% correspondence to the severity of RA was estimated by a logistic regression model and statistical significance was estimated by Fisher's exact test. Probability values of less than 0.05 were considered statistically significant. All statistical analyses were carried out with SAS software version 9.1.3 (SAS Institute, Cary, NC, USA).

Results

Clinical and biochemical characteristics of the study subjects

There were no significant differences between mild and severe RA groups in age (60.8±11.0 vs. 61.7±11.7 years), disease duration (15.5±6.9 vs. 17.3±6.8 years), body mass index (22.1±3.4 vs. 20.8±3.0 kg/m^2), and prevalence of hypertension (18.8% vs. 28.3%), diabetes (16.2 vs. 18.9%), and hyperlipidemia (21.6 vs. 24.5%). The age and BMI of subjects of the control group were 61.0±11.4 years and 21.9±3.2 kg/m^2, respectively. The prevalence of each

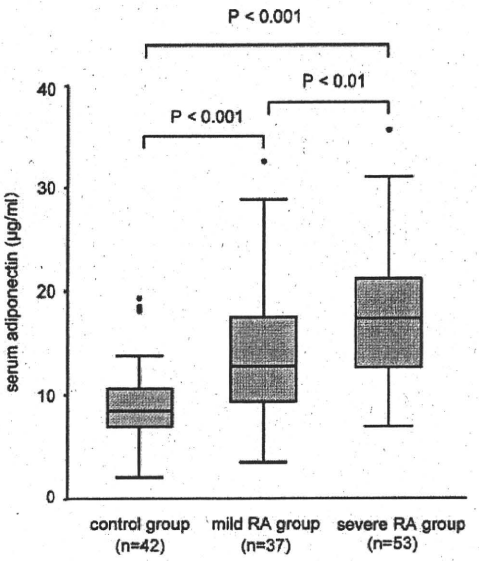

Fig. 1 Box-and-whisker plots of serum adiponectin levels in the control group, mild RA group, and severe RA group evaluated by the number of joint destruction in 68 joints on plain radiograph. The mean serum level of adiponectin was significantly higher in the severe RA group (17.7±6.7 μg/ml) than in the control (9.1±3.8 μg/ml) or mild RA group (13.9±6.5 μg/ml) (control vs. mild RA group: $P<0.001$, mild RA vs. severe RA group: $P<0.01$, control vs. severe RA group: $P<0.001$)

Table 1 Baseline demographic, laboratory, and clinical characteristics of the two RA groups

	mild RA group (n=37)	severe RA group (n=53)	P^a value
Age, years	60.8±11.0	61.7±11.7	NS
Duration of disease, years	15.5±6.9	17.3±6.8	NS
Body mass index, kg/m^2	22.1±3.4	20.8±3.0	NS
CRP, mg/l	0.9±1.3	1.9±2.0	0.003
MMP-3, ng/ml	146.5±150.9	222.8±177.6	0.047
IL-6, ρg/ml	14.5±36.0	18.1±26.2	NS
RF titer, IU/ml	158.1±417.0	235.7±366.9	NS
RF positivity, % patients	77.1%	82.7%	NS[b]
BAP, U/l	24.0±13.5	23.9±9.5	NS
iOC, ng/ml	6.9±3.5	6.7±7.3	NS
1CTP, ng/ml	4.9±1.9	6.5±3.1	0.010
uDPD, nmol/mmol creatinine	6.6±2.2	7.9±3.2	NS
DAS28-CRP	2.2±1.0	3.1±1.5	0.001
Prednisolone dosage, mg/day	2.2±2.5	4.3±3.6	0.001
Methotrexate dosage, mg/week	4.3±3.2	4.4±3.6	NS
Adiponectin, μg/ml	13.9±6.5	17.7±6.7	0.008

Data are mean ± SD

RA rheumatoid arthritis, *NS* not significant, *CRP* C-reactive protein, *MMP-3* matrix metalloproteinase-3, *IL-6* interleukin-6, *RF* rheumatoid factor, *BAP* bone-specific alkaline phosphatase, *iOC* intact osteocalcin, *1CTP* pyridinoline cross-linked carboxyterminal telopeptide of type 1 collagen, *uDPD* urinary deoxypyridinoline, *DAS28-CRP* disease activity score including a 28-joint count/CRP

[a] Except where otherwise indicated, determined by Mann–Whitney *U* test

[b] Except where otherwise indicated, determined by chi-square test

Table 2 Spearman's correlation analysis of the relation between serum adiponectin and other variables in all RA patients

Variable	*r* value	*P* value
Age, years	0.046	NS
Duration of disease, years	0.068	NS
Body mass index, kg/m^2	−0.269	0.011
CRP, mg/liter	0.078	NS
MMP-3, ng/ml	0.098	NS
IL-6, ρg/ml	0.120	NS
RF titer, IU/ml	−0.033	NS
BAP, U/l	−0.193	NS
iOC, ng/ml	−0.075	NS
1CTP, ng/ml	0.033	NS
uDPD, nmol/mmol creatinine	−0.002	NS
DAS28-CRP	0.096	NS
Prednisolone dosage, mg/day	0.040	NS

r value Spearman's rank correlation coefficient, *NS* not significant, *CRP* C-reactive protein, *MMP-3* matrix metalloproteinase-3, *IL-6* interleukin-6, *RF* rheumatoid factor, *BAP* bone-specific alkaline phosphatase, *iOC* intact osteocalcin, *1CTP* pyridinoline cross-linked carboxyterminal telopeptide of type 1 collagen, *uDPD* urinary deoxypyridinoline, *DAS28-CRP* disease activity score including a 28-joint count/CRP

Table 3 Results of Spearman's rank correlation analysis of the relation between adiponectin and other variables with a significant difference between the severe and mild RA groups

	CRP	MMP-3	1CTP	DAS28-CRP	Prednisolone	Adiponectin
CRP		0.574***	0.486***	0.717***	0.335**	0.078
MMP-3			0.331**	0.532***	0.510***	0.098
1CTP				0.389***	0.220*	0.033
DAS28-CRP					0.372**	0.096
Prednisolone						0.040

CRP C-reactive protein, *MMP-3* matrix metalloproteinase-3, *1CTP* pyridinoline cross-linked carboxyterminal telopeptide of type 1 collagen, *DAS28-CRP* disease activity score including a 28-joint count/CRP
*$P<0.05$; **$P<0.01$; ***$P<0.001$

disease in the control group was 0% for hypertension, 2.3% for diabetes, and 9.5% for hyperlipidemia. Patients of the severe RA group had a significantly higher serum C-reactive protein (CRP) ($P=0.003$), matrix metalloproteinase (MMP)-3 ($P=0.047$), pyridinoline cross-linked carboxyterminal telopeptide of type 1 collagen (1CTP) ($P=0.010$), disease activity score including a 28-joint count/CRP (DAS28-CRP) ($P=0.001$), and prednisolone dose ($P=0.001$) than the mild RA group (Table 1), reflecting high inflammatory state and bone resorption level in this group as described previously [24]. The mean serum level of adiponectin was significantly higher in the total RA group (16.1±6.8 μg/ml) than in the control group (9.1±3.8 μg/ml) ($P<0.001$). Moreover, the mean serum level of adiponectin was significantly higher in the severe RA group (17.7±6.7 μg/ml) than in the control (9.1±3.8 μg/ml) or mild RA group (13.9±6.5 μg/ml) (control vs. mild RA group, $P<0.001$; mild RA vs. severe RA group, $P<0.01$, control vs. severe RA group, $P<0.001$) (Fig. 1). Univariate analysis of the relationship between serum adiponectin level and other variables showed that adiponectin correlated negatively with BMI ($r=-0.269$, $P=0.011$), but did not correlate with other variables such as inflammatory markers, bone metabolism markers, DAS28-CRP, or the dose of prednisolone (Table 2). Calculation of Spearman's rank correlation coefficients for the variables with a significant difference between the mild and severe RA groups showed that CRP correlated with MMP-3 ($r=0.574$, $P<0.001$), 1CTP ($r=0.486$, $P<0.001$), DAS28-CRP($r=0.717$, $P<0.001$), and dose of prednisolone ($r=0.335$, $P<0.01$), while there was no significant correlation with adiponectin ($r=0.078$, $P>0.05$) (Table 3). In addition, the dose of prednisolone correlated with CRP, MMP-3, 1CTP, and DAS28-CRP, but not with adiponectin ($r=0.040$, $P>0.05$) (Table 3). Multivariate logistic regression analyses revealed that even when the odds ratios were adjusted for BMI, serum adiponectin level significantly correlates with disease severity of RA ($P=0.031$) (Table 4).

Cutoff point of serum adiponectin for severe RA

Figure 2 shows the histogram of serum adiponectin levels of patients of the mild and severe RA groups. For clinical translation, the cutoff levels were selected. The cutoff value for serum adiponectin level was estimated at 18 μg/ml, yielding 80% correspondence with the severity of RA. Among the patients with serum adiponectin level of ≥18 μg/ml, 81.3% (26/32) belonged to the severe RA group and 18.8% (6/32) belonged to the mild RA group. This cutoff line showed significant correlation with disease severity ($P<0.01$). The specificity of this cutoff value was 53.4% (31/58) (Table 5).

Changes in serum adiponectin levels and severity of RA during follow-up

To further investigate the time-course changes of serum adiponectin levels and severity of RA, 18 patients underwent a second assessment 2.5 years later (Fig. 3). The mean serum adiponectin level of all patients did not change significantly, although it showed tendency to increase (14.0±5.5 to 15.2±5.2 μg/ml; $P=0.07$). Furthermore, the mean serum adiponectin level did not change significantly within the RA group (10.8±5.8 to 12.4±5.8 μg/ml in the mild RA group, $P=0.122$ and 17.2±2.7 to 18.0±2.4 μg/ml in the severe RA group, $P=0.372$). Assessment of RA severity revealed that none of the mild RA patients progressed to severe RA (data not shown).

Table 4 Adjusted ORs of serum adiponectin level and BMI for disease severity of RA

	Adjusted OR	95% CI	*P* value
Adiponectin, μg/ml	1.085	1.007–1.168	0.031
BMI, kg/m^2	0.907	0.785–1.048	NS

ORs odds ratios, *95% CI* 95% confidence interval, *NS* not significant

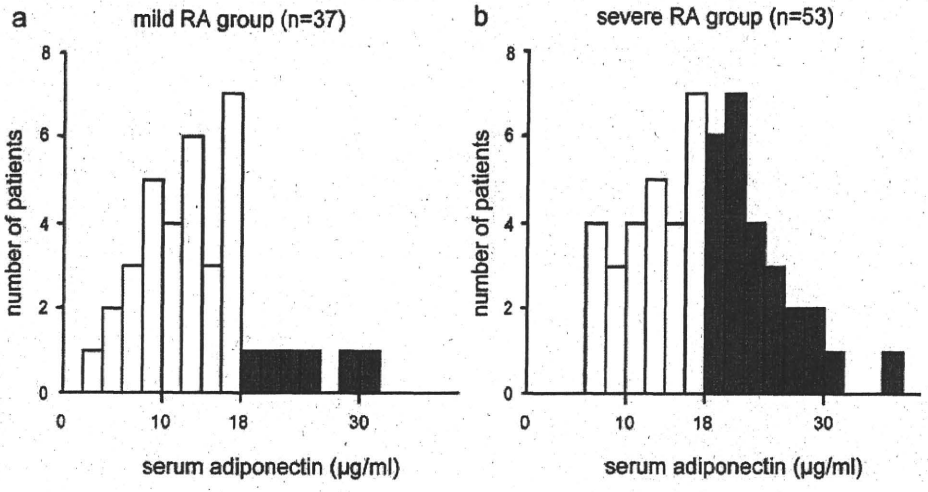

Fig. 2 Histograms showing the distribution of serum adiponectin levels in mild RA group (a) and severe RA group (b). Each column covers a serum adiponectin range of 2 μg/ml. When the cutoff value for adiponectin was set at 18 μg/ml, there was 80% correspondence with the severity of RA. Among patients with serum adiponectin levels ≥18 μg/ml, 81.3% (26/32) belonged to the severe RA group and 18.8% (6/32) belonged to the mild RA group

Discussion

The long-term functional prognosis of RA patients in daily life is mainly determined by the extent of damage in large joints such as the hip, knee, ankle, subtalar, shoulder, and elbow joints, rather than in small joints of the hands or feet. A previous report using Ochi's method demonstrated that MES and MUD groups underwent higher frequency of total knee or hip replacement than LES group (54.7% vs. 0.5%) [25], suggesting that Ochi's method offers some advantages for assessing large joint destruction [20, 25–27]. Therefore, we used Ochi's method to evaluate the severity of RA, to investigate the factors associated with the extent of overall joint destruction, especially in large joints [20]. Evaluation using this method revealed that markers associated with RA activity, such as CRP, MMP-3, 1CTP, and DAS28-CRP were all significantly higher in the severe RA group than in the mild RA group. These results were in agreement with previously published reports evaluated by the modified Sharp/van der Heijde method and Larsen's method (CRP [28], MMP-3 [29], 1CTP [30], and DAS [31]).

We showed for the first time that serum adiponectin levels were higher in the severe RA group than in control and mild RA groups. Interestingly, while other disease severity-related variables, such as MMP-3, 1CTP, DAS28-CRP, and dose of prednisolone correlated with CRP, serum adiponectin levels did not, in both the mild and severe RA groups (Table 3). It has been reported that serum TNF-α and CRP levels are elevated in RA patients [32, 33], and TNF-α, CRP, and corticosteroid markedly inhibit adiponectin gene expression in cultured adipocytes [16, 34]. Furthermore, anti-TNF-α therapy restored serum adiponectin level in RA patients [14, 15, 35]. On the other hand, despite elevated CRP levels and higher dose of treated oral prednisolone (corticosteroid), serum adiponectin levels were elevated in the severe RA group than in the mild

Table 5 Separation of mild and severe RA using a cutoff value for serum adiponectin of 18 μg/ml

	Serum adiponectin level	
	<18 μg/ml	≥18 μg/ml
Mild RA group (n)	31	6
Severe RA group (n)	27	26
% with severe RA	46.6%	81.3%

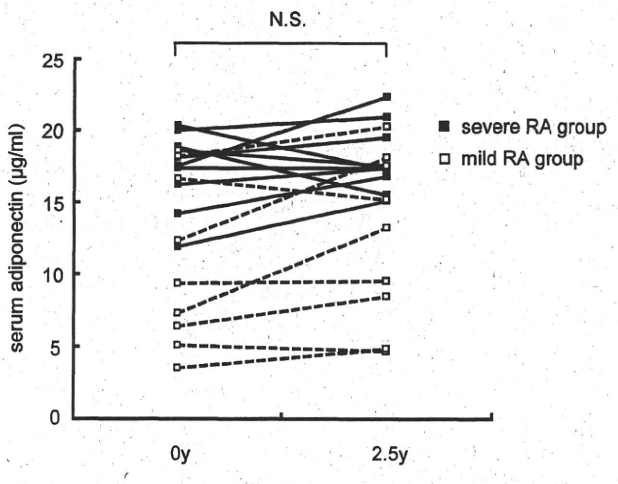

Fig. 3 Changes in serum adiponectin levels of 18 RA subjects in 2.5-year interval. The mean serum adiponectin level of the whole group was 14.0±5.5 μg/ml at baseline (0 years) and 15.2±5.2 μg/ml at follow-up (2.5 years, P=0.07); 10.8±5.8 vs. 12.4±5.8 μg/ml in mild RA group (P=0.122) and 17.2±2.7 vs. 18.0±2.4 μg/ml in severe RA group (P=0.372) and the change was not significant in either groups. None of the mild RA patients showed worsening to severe RA category during this period

RA group in the present study (Table 3). Considered together, serum adiponectin should be induced by unknown factors associated with the number of destructed joints, especially in large joints, and their effects should exceed the inhibitory effects of TNF-α, CRP, and prednisolone in RA patients. Recently, Fantuzzi [36] suggested that adiponectin promotes survival during periods of catabolism secondary to malnutrition and that hyperadiponectinemia may be the result of response to catabolic state in RA. Consequently, a catabolic state accompanied by joint destruction, especially in large joints, may be one of the strong inducer of serum adiponectin level.

It has been reported that a low BMI is a sensitive and independent predictor of radiographic progression of joint damage assessed by Larsen's method in RA [37, 38]. In this study, there was no significant difference in BMI between control, mild RA, and severe RA group (21.9±3.2 vs. 22.1± 3.4 vs. 20.8±3.0 kg/m^2). In addition, in total RA group, BMI showed only tendency of positive correlation with disease severity (P=0.059). However, under such condition, serum adiponectin levels were significantly higher in severe RA group than in the control and mild RA groups (Table 1, Fig. 1). Furthermore, multivariate logistic regression analyses revealed that even when the odds ratios were adjusted for BMI, serum adiponectin level significantly correlates with disease severity of RA (Table 4). Therefore, we speculate that serum adiponectin levels can be a better sensitive indicator of the expansion of joint destruction than BMI in RA patients. To further investigate the time course changes in serum adiponectin levels and severity of RA, 18 patients were assessed 2.5 years later. The results showed no significant change in serum adiponectin levels and none of the mild RA patients progressed to severe RA. The lack of change in the severity category during this period is compatible with previous reports indicating that most of the progression of joint damage in RA occurs during the first years of the disease and decrease thereafter [10, 11, 20]; and under such conditions, serum adiponectin level is relatively stable in established RA (disease duration ≥5 years).

For clinical translation of these findings, we determined the cutoff level of serum adiponectin level. The estimated cutoff levels estimated by the histogram of serum adiponectin level showed relatively high sensitivity (81.3%) but low specificity (53.4%) in this study (Fig. 2, Table 5), indicating that increased number of destructed joints may be one of the additive, but not a specific factor of high serum adiponectin level in RA. Consequently, prospective studies in early stage of RA (disease duration <5 years) and in large number of RA patients are needed to determine the cutoff level of adiponectin to be used as an indicator or predictor of destructed joints. In addition, to elucidate the effect of hyperadiponectinemia on the severity of RA, further animal experiments are needed.

Despite the limitation of observational study, we demonstrated that the severity of RA, evaluated by the number of destructed joints on plain radiographs detected in the whole skeleton, correlated with serum adiponectin concentrations. This finding should encourage further research to investigate the role of adiponectin in RA and design new adiponectin-based treatment strategies for RA.

Acknowledgments This work was supported by grants from the Ministry of Health, Labor, and Welfare of Japan.

Disclosures None.

References

1. Maeda N, Shimomura I, Kishida K, Nishizawa H, Matsuda M, Nagaretani H, Furuyama N, Kondo H, Takahashi M, Arita Y, Komuro R, Ouchi N, Kihara S, Tochino Y, Okutomi K, Horie M, Takeda S, Aoyama T, Funahashi T, Matsuzawa Y (2002) Diet-induced insulin resistance in mice lacking adiponectin/ACRP30. Nat Med 8:731–737
2. Matsuda M, Shimomura I, Sata M, Arita Y, Nishida M, Maeda N, Kumada M, Okamoto Y, Nagaretani H, Nishizawa H, Kishida K, Komuro R, Ouchi N, Kihara S, Nagai R, Funahashi T, Matsuzawa Y (2002) Role of adiponectin in preventing vascular stenosis. The missing link of adipo-vascular axis. J Biol Chem 277:37487–37491
3. Wulster-Radcliffe MC, Ajuwon KM, Wang J, Christian JA, Spurlock ME (2004) Adiponectin differentially regulates cytokines in porcine macrophages. Biochem Biophys Res Commun 316:924–929
4. Luo XH, Guo LJ, Yuan LQ, Xie H, Zhou HD, Wu XP, Liao EY (2005) Adiponectin stimulates human osteoblasts proliferation and differentiation via the MAPK signaling pathway. Exp Cell Res 309:99–109
5. Oshima K, Nampei A, Matsuda M, Iwaki M, Fukuhara A, Hashimoto J, Yoshikawa H, Shimomura I (2005) Adiponectin increases bone mass by suppressing osteoclast and activating osteoblast. Biochem Biophys Res Commun 331:520–526
6. Otero M, Lago R, Gomez R, Lago F, Dieguez C, Gomez-Reino JJ, Gualillo O (2006) Changes in plasma levels of fat-derived hormones adiponectin, leptin, resistin and visfatin in patients with rheumatoid arthritis. Ann Rheum Dis 65:1198–1201
7. Senolt L, Pavelka K, Housa D, Haluzik M (2006) Increased adiponectin is negatively linked to the local inflammatory process in patients with rheumatoid arthritis. Cytokine 35:247–252
8. Ehling A, Schaffler A, Herfarth H, Tarner IH, Anders S, Distler O, Paul G, Distler J, Gay S, Scholmerich J, Neumann E, Muller-Ladner U (2006) The potential of adiponectin in driving arthritis. J Immunol 176:4468–4478
9. Arita Y, Kihara S, Ouchi N, Takahashi M, Maeda K, Miyagawa J, Hotta K, Shimomura I, Nakamura T, Miyaoka K, Kuriyama H, Nishida M, Yamashita S, Okubo K, Matsubara K, Muraguchi M, Ohmoto Y, Funahashi T, Matsuzawa Y (1999) Paradoxical decrease of an adipose-specific protein, adiponectin, in obesity. Biochem Biophys Res Commun 257:79–83
10. Sharp JT, Wolfe F, Mitchell DM, Bloch DA (1991) The progression of erosion and joint space narrowing scores in rheumatoid arthritis during the first twenty-five years of disease. Arthritis Rheum 34:660–668

11. van der Heijde DM, van Leeuwen MA, van Riel PL, Koster AM, van 't Hof MA, van Rijswijk MH, van de Putte LB (1992) Biannual radiographic assessments of hands and feet in a three-year prospective followup of patients with early rheumatoid arthritis. Arthritis Rheum 35:26–34
12. Arnett FC, Edworthy SM, Bloch DA, McShane DJ, Fries JF, Cooper NS, Healey LA, Kaplan SR, Liang MH, Luthra HS et al (1988) The American Rheumatism Association 1987 revised criteria for the classification of rheumatoid arthritis. Arthritis Rheum 31:315–324
13. Ryo M, Nakamura T, Kihara S, Kumada M, Shibazaki S, Takahashi M, Nagai M, Matsuzawa Y, Funahashi T (2004) Adiponectin as a biomarker of the metabolic syndrome. Circ J 68:975–981
14. Komai N, Morita Y, Sakuta T, Kuwabara A, Kashihara N (2007) Anti-tumor necrosis factor therapy increases serum adiponectin levels with the improvement of endothelial dysfunction in patients with rheumatoid arthritis. Mod Rheumatol 17:385–390
15. Nishida K, Okada Y, Nawata M, Saito K, Tanaka Y (2008) Induction of hyperadiponectinemia following long-term treatment of patients with rheumatoid arthritis with infliximab (IFX), an anti-TNF-alpha antibody. Endocr J 55:213–216
16. Fasshauer M, Klein J, Neumann S, Eszlinger M, Paschke R (2002) Hormonal regulation of adiponectin gene expression in 3T3-L1 adipocytes. Biochem Biophys Res Commun 290:1084–1089
17. Maeda N, Takahashi M, Funahashi T, Kihara S, Nishizawa H, Kishida K, Nagaretani H, Matsuda M, Komuro R, Ouchi N, Kuriyama H, Hotta K, Nakamura T, Shimomura I, Matsuzawa Y (2001) PPARgamma ligands increase expression and plasma concentrations of adiponectin, an adipose-derived protein. Diabetes 50:2094–2099
18. Yamada S, Ano N, Toda K, Kitaoka A, Shiono K, Inoue G, Atsuda K, Irie J (2008) Telmisartan but not candesartan affects adiponectin expression in vivo and in vitro. Hypertens Res 31:601–606
19. Koshiba K, Nomura M, Nakaya Y, Ito S (2006) Efficacy of glimepiride on insulin resistance, adipocytokines, and atherosclerosis. J Med Invest 53:87–94
20. Ochi T, Yonemasu K, Iwase R, Sasaki T, Tsuyama K, Ono K (1984) Serum C1q levels as a prognostic guide to articular erosions in patients with rheumatoid arthritis. Arthritis Rheum 27:883–887
21. Steinbrocker O, Traeger CH, Batterman RC (1949) Therapeutic criteria in rheumatoid arthritis. J Am Med Assoc 140:659–662
22. Wakitani S, Murata N, Toda Y, Ogawa R, Kaneshige T, Nishimura Y, Ochi T (1997) The relationship between HLA-DRB1 alleles and disease subsets of rheumatoid arthritis in Japanese. Br J Rheumatol 36:630–636
23. Inoue E, Yamanaka H, Hara M, Tomatsu T, Kamatani N (2007) Comparison of Disease Activity Score (DAS)28- erythrocyte sedimentation rate and DAS28-C-reactive protein threshold values. Ann Rheum Dis 66:407–409
24. Toritsuka Y, Nakamura N, Lee SB, Hashimoto J, Yasui N, Shino K, Ochi T (1997) Osteoclastogenesis in iliac bone marrow of patients with rheumatoid arthritis. J Rheumatol 24:1690–1696
25. Wakitani S, Kuwata K, Imoto K, Murata N, Oonishi H, Ochi T (1998) Knee and/or hip joint destruction in rheumatoid arthritis is associated with HLA-DRB1*0405 in Japanese patients. Clin Rheumatol 17:485–488
26. Momohara S, Yamanaka H, Holledge MM, Mizumura T, Ikari K, Okada N, Kamatani N, Tomatsu T (2004) Cartilage oligomeric matrix protein in serum and synovial fluid of rheumatoid arthritis: potential use as a marker for joint cartilage damage. Mod Rheumatol 14:356–360
27. Shibuya K, Hagino H, Morio Y, Teshima R (2002) Cross-sectional and longitudinal study of osteoporosis in patients with rheumatoid arthritis. Clin Rheumatol 21:150–158
28. Jansen LM, van der Horst-Bruinsma IE, van Schaardenburg D, Bezemer PD, Dijkmans BA (2001) Predictors of radiographic joint damage in patients with early rheumatoid arthritis. Ann Rheum Dis 60:924–927
29. Young-Min S, Cawston T, Marshall N, Coady D, Christgau S, Saxne T, Robins S, Griffiths I (2007) Biomarkers predict radiographic progression in early rheumatoid arthritis and perform well compared with traditional markers. Arthritis Rheum 56:3236–3247
30. Aman S, Paimela L, Leirisalo-Repo M, Risteli J, Kautiainen H, Helve T, Hakala M (2000) Prediction of disease progression in early rheumatoid arthritis by ICTP, RF and CRP. A comparative 3-year follow-up study. Rheumatology (Oxford) 39:1009–1013
31. Welsing PM, van Gestel AM, Swinkels HL, Kiemeney LA, van Riel PL (2001) The relationship between disease activity, joint destruction, and functional capacity over the course of rheumatoid arthritis. Arthritis Rheum 44:2009–2017
32. Barrera P, Boerbooms AM, Janssen EM, Sauerwein RW, Gallati H, Mulder J, de Boo T, Demacker PN, van de Putte LB, van der Meer JW (1993) Circulating soluble tumor necrosis factor receptors, interleukin-2 receptors, tumor necrosis factor alpha, and interleukin-6 levels in rheumatoid arthritis. Longitudinal evaluation during methotrexate and azathioprine therapy. Arthritis Rheum 36:1070–1079
33. Cohick CB, Furst DE, Quagliata S, Corcoran KA, Steere KJ, Yager JG, Lindsley HB (1994) Analysis of elevated serum interleukin-6 levels in rheumatoid arthritis: correlation with erythrocyte sedimentation rate or C-reactive protein. J Lab Clin Med 123:721–727
34. Yuan G, Chen X, Ma Q, Qiao J, Li R, Li X, Li S, Tang J, Zhou L, Song H, Chen M (2007) C-reactive protein inhibits adiponectin gene expression and secretion in 3T3-L1 adipocytes. J Endocrinol 194:275–281
35. Serelis J, Kontogianni MD, Katsiougiannis S, Bletsa M, Tektonidou MG, Skopouli FN (2008) Effect of anti-TNF treatment on body composition and serum adiponectin levels of women with rheumatoid arthritis. Clin Rheumatol 27:795–797
36. Fantuzzi G (2008) Adiponectin and inflammation: consensus and controversy. J Allergy Clin Immunol 121:326–330
37. van der Helm-van Mil AH, van der Kooij SM, Allaart CF, Toes RE, Huizinga TW (2008) A high body mass index has a protective effect on the amount of joint destruction in small joints in early rheumatoid arthritis. Ann Rheum Dis 67:769–774
38. Westhoff G, Rau R, Zink A (2007) Radiographic joint damage in early rheumatoid arthritis is highly dependent on body mass index. Arthritis Rheum 56:3575–3582

201023002B (2/2)

厚生労働科学研究費補助金

免疫アレルギー疾患等予防・治療研究事業

関節リウマチ骨髄血中の疾患誘導因子解明と根治療法開発研究

平成２０年度～平成２２年度　総合研究報告書

（２／２分冊）

研究代表者　越　智　隆　弘

平成２３（２０１１）年３月

Analysis of Radiocarpal and Midcarpal Motion in Stable and Unstable Rheumatoid Wrists Using 3-Dimensional Computed Tomography

Sayuri Arimitsu, MD, Kazuomi Sugamoto, MD, PhD, Jun Hashimoto, MD, PhD, Tsuyoshi Murase, MD, PhD, Hideki Yoshikawa, MD, PhD, Hisao Moritomo, MD, PhD

Purpose The kinematic evaluation of carpal motion, especially midcarpal motion, in rheumatoid arthritis (RA) has been extremely difficult because of limited imaging techniques previously available. The purpose of this study was to evaluate the amount of radiocarpal and midcarpal motion in the flexion-extension plane in both stable and unstable rheumatoid wrists using three-dimensional computed tomography.

Methods We acquired *in vivo* kinematic data on 30 wrists with RA by three-dimensional computed tomography with the wrist in 3 positions: neutral, maximum flexion, and maximum extension. All cases were radiographically classified into 1 of 2 subtypes, the stable form or unstable form, according to the classification by Flury et al. We evaluated the precise range of radiocarpal and midcarpal motion using a markerless bone registration technique and calculated the individual contributions to the total amount of wrist motion in the flexion-extension plane in the different radiographic subtypes of RA.

Results The average range of motion of radiocarpal and midcarpal joint was 27° ± 15 and 32° ± 17, respectively. The average contribution of midcarpal motion to the total amount of wrist motion was 54%. The average contribution of midcarpal motion in the unstable form was 67%, which was significantly higher than 47% ($p < .05$) in the stable form.

Conclusions Midcarpal motion of rheumatoid wrists in the flexion-extension plane was better preserved than previously thought. The contribution of midcarpal motion to the total amount of wrist motion was significantly greater ($p < .05$) in the unstable form than in the stable form of RA. *(J Hand Surg 2008;33A:189–197. Copyright © 2008 by the American Society for Surgery of the Hand.)*

Key words Kinematics, rheumatoid arthritis, three-dimensional, wrist.

Additional material is available online.

THE INVOLVEMENT OF THE WRIST in rheumatoid arthritis (RA) is common, and surgical treatment is often required to alleviate persistent wrist pain. The natural course of destruction in a rheumatoid wrist has been classified into 3 types by Simmen and Huber[1]: type I, the ankylosis type; type II, the osteoarthritis type; and type III, the disintegrating type. Based on their radiologic analysis, type I has a spontaneous tendency to progress into ankylosis, type II resembles secondary osteoarthritic changes as destruction progresses, and type III has progressive destruction, loss of alignment, and finally complete collapse of the wrist.[1] In addition, Flury et al[2] proposed the classification of wrists with RA into a stable form of the disease (types I and II) and an unstable form of disease (type III) to make the choice and timing of surgical intervention easier (Table 1 and Fig. 1). It has generally been thought that the deterioration of midcarpal joint is more severe in the unstable form than in the stable form.[3] Therefore, the partial arthrodesis technique, like radiolunate (RL) arthrodesis, has been applicable to the stable form, whereas the unstable form has been better treated by total arthrodesis of the wrist.[3]

Radiolunate arthrodesis is a well-established procedure for the RA wrists, and several researchers have reported the favorable clinical results of the procedure.[2–12] It has been suggested that RL arthrodesis is most useful in those

Department of Orthopaedic Surgery, Osaka University Graduate School of Medicine, Osaka, Japan.

The authors acknowledge the assistance during parts of the experimental procedure of Tetsuya Tomita, MD, PhD, Akira Goto, MD, PhD, Kunihiro Oka, MD, PhD, and Ryoji Nakao, Department of Orthopaedic Surgery, Osaka University Graduate School of Medicine.

Received for publication June 13, 2007; accepted in revised form November 15, 2007.

The authors received support from the Japan Science and Technology Agency.

Corresponding author: Sayuri Arimitsu, MD, Department of Orthopaedic Surgery, Osaka University Graduate School of Medicine, 2-2, Yamada-oka, Suita, Osaka 565-0871, Japan; e-mail: sayu@df6.so-net.ne.jp.

0363-5023/08/33A02-0007$34.00/0
doi:10.1016/j.jhsa.2007.11.012

TABLE 1: Classification by the Natural Course of the Rheumatoid Wrist and the Radiologic Parameters Described by Simmen and Huber and Flury et al

	Classification		Radiologic Parameters	
	Simmen and Huber[1]	Flury et al[2]	Ulnar Carpal Translocation* (mm)	Loss of Carpal Height Ratio*
Type I	Ankylosis	Stable form	3.7 (0–11)	Δ0.14 (0.01–0.28)
Type II	Osteoarthritis	Stable form	3.8 (0–8)	Δ0.16 (0.02–0.34)
Type III	Disintegration	Unstable form	9.5 (4–17)	Δ0.30 (0.10–0.46)

*The radiologic parameters 10 to 20 years after onset of RA represented by Simmen and Huber[1] (n = 126).

rheumatoid patients whose disease had left the midcarpal joints relatively unaffected as seen on the radiograph.[1] However, the preoperative evaluation of the midcarpal joint on the radiograph has been difficult because of the complicated and overlapping shapes of the carpal bones in RA deformities. Recently, researchers have been able to measure *in vivo* and three-dimensional (3-D) kinematics of the human joint using a markerless bone registration technique, which is a method for evaluating the precise motions by determining relative positions of bones in different volume images.[13–19] We thought it would be possible to evaluate the kinematics of the carpal motion and quantify the midcarpal motion preoperatively in cases of RA with this 3-D technique.

The kinematic behavior of the carpal bones in rheumatoid wrist is not well-known, especially in relation to the RA subtypes. The purpose of this study was to evaluate the amount of radiocarpal and midcarpal motion in the flexion-extension plane in both stable and unstable rheumatoid wrists using 3-D computed tomography (3-D CT). We calculated the individual contributions of radiocarpal and midcarpal motion to the total amount of wrist motion to determine which radiographic subtype of RA had the greater contribution of midcarpal motion to the total amount of wrist motion.

MATERIALS AND METHODS

Subjects

We randomly selected 30 wrists from 29 RA patients who were regularly treated with medication at our institution. All of them had pain and instability of the wrists. One patient was a man and 28 were women. The average age was 60 years (range, 21 to 80 years). The average duration of RA was 13 years (range, 6 to 38 years). For comparison, we investigated a control group of 10 normal wrists from 10 healthy volunteers comprising 8 men and 2 women whose average age was 29 years (range, 22 to 36 years). All subjects consented to be included in this study.

Radiographic Evaluation

To investigate the relationship between the contribution of midcarpal motion to the total amount of wrist motion and the radiographic appearance of RA, we classified 30 wrists with RA into 1 of the 2 subtypes, the stable form or the unstable form of the disease, by the natural course of the rheumatoid wrist and the radiologic parameters (Table 1 and

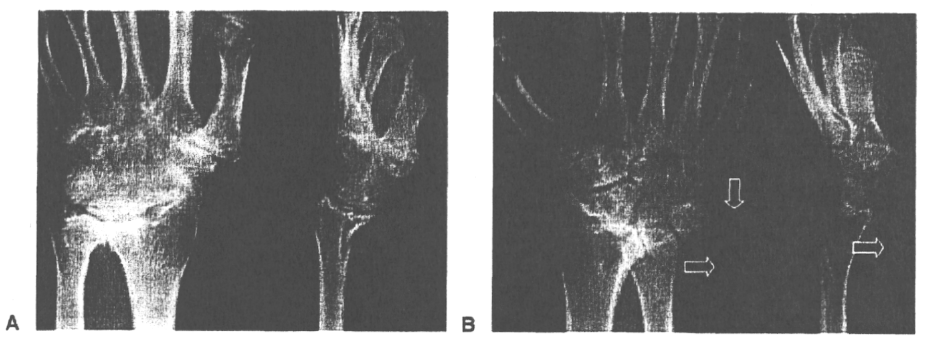

FIGURE 1: The A stable form and B unstable form of RA by the method of Flury et al.[2] A Representative case of the stable form of RA, which has a spontaneous tendency to progress into ankylosis (Video 1, a 3-dimensional animation of a representative case of the stable form of RA wrist, may be viewed at the *Journal's* Web site, www.jhandsurg.org). B Representative case of the unstable form of RA in which there is progressive destruction and loss of alignment. The carpal height is reduced and the carpal bones are dislocated ulno-palmarly with respect to the case shown in A (arrows) (Video 2, a 3-dimensional animation of a representative case of the unstable form of RA wrist, may be viewed at the *Journal's* Web site, www.jhandsurg.org).

Fig. 1).[1,2] The radiographic parameters we used for classification were ulnar translocation and carpal height ratio (Table 1).[1] In the current study, we also investigated our cases with or without scaphoid-lunate (S-L) dissociation (the gap between scaphoid and lunate is more than 2 mm[12] on the anteroposterior radiograph) in relation to the radiographic subtypes of RA.

Image Acquisition

The technique we used for *in vivo* 3-D kinematic evaluation has been described in detail previously.[14–19] For patients with RA, we performed 3-D CT on the wrists using a clinical helical type scanner with an image slice thickness of 0.625 mm (LightSpeed Ultra16; General Electric, Waukesha, WI). For the normal wrists of volunteers, magnetic resonance images were obtained using a 1.5-T commercial magnetic resonance imaging (MRI) system (Magnetom Vision PlusR 1.5T MRI; Siemens, Munich, Germany) in conjunction with a receive-only surface coil of 2.3 ms/33 ms, a flip angle of 45°, a 160-mm field of view, and 0.5-mm-thick contiguous slices, with 0.6 × 0.8 mm pixels. For each wrist, we acquired image with the wrist in 3 different positions: neutral (in which the third metacarpal and the forearm axis were aligned), maximum wrist flexion, and maximum wrist extension. For normal volunteers, we used a custom-made device to hold the position during image acquisition. However, we could not use the device for RA patients because of pain and deformity of the wrists. Data were saved in a standard format (Digital Imaging and Communications in Medicine [DICOM]) that is used commonly for transferring and storing medical images.

Segmentation and Construction of a 3-D Surface Bone Model

Segmentation was defined as extracting bone regions individually. The anatomic structure or region of interest must be delineated and separated so that it can be viewed individually and 3-D bone models can be reconstructed. Regions of individual bones were segmented semiautomatically using a software program for image analysis (Virtual Place-M; AZE, Ltd., Tokyo, Japan). The software generated 3-D surface bone models using the marching cubes technique.[14,15,20]

Registration

We created 3-D bone models and quantitatively evaluated the motion of the midcarpal joint using a markerless volume-based registration technique. The kinematic variables were calculated by registering the bone, obtained by segmentation, from one position to another. The accuracy of volume-based registration has been discussed previously,[14,15] the mean rotation error was 1° ± 1, and the mean translation error was 0.21 mm ± 0.25.

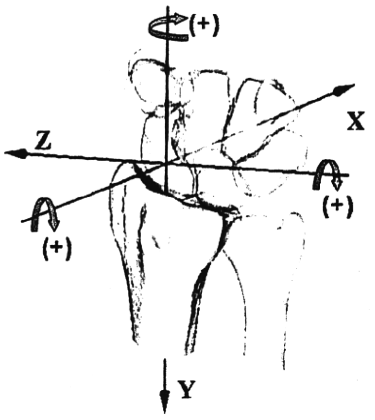

FIGURE 2: A consistent orthogonal reference system established in the radius.

Three-Dimensional Quantification of the Range of Motion

To quantify the 3-D range of motion of the midcarpal joint, we defined the grid for the radius, which was the orthogonal reference system advocated by Belsole et al (Fig. 2).[15,21,22] The total amount of wrist motion in the flexion-extension plane was defined as the total range of motion of the radiocarpal and midcarpal joint in the flexion-extension plane, which was evaluated by assessing the range of capitate motion relative to the reference system established on the radius. The range of radiocarpal motion in the flexion-extension plane was investigated by that of the lunate motion. Then the range of the midcarpal motion in the flexion-extension plane could be quantified as the difference between the total amount of wrist motion and the range of radiocarpal motion.

In the flexion-extension motion of the wrist, the radiocarpal and midcarpal joints have motions in planes other than the flexion-extension plane such as the pronation/supination (P/S) plane and the radial/ulnar deviation (RD/UD) plane. There are coupling motions associated with wrist motion in the flexion-extension plane. We defined the 2 motions in the other planes as *out of the plane motion (P/S)* and *out of the plane motion (RD/UD)*, respectively. We quantified the amount of wrist motion in the flexion-extension plane and out of the plane separately for the radiocarpal and midcarpal joints.

A consistent orthogonal reference system was established in the radius as follows.[22] The y axis was defined as the longitudinal radial axis and indicated the proximal (+)/distal (–) direction. The z axis was defined as the line running through the styloid process on the plane perpendicular to the y axis and indicated the radial (+)/ulnar (–) direction. The x axis was defined as the line perpendicular to the yz plane and indicated the palmar (+)/dorsal (–) direction. Rotation around the z axis produced flexion (+)/extension (–), rotation around the y axis was pronation (+)/supination (–), and rotation around the x axis was ulnar (+)/radial (–)

deviation (Fig. 2). We defined the rotating angle of the carpus around each of the 3 axes as the range of wrist motion.

Evaluation of the Contribution Ratio

We also evaluated the individual contributions of radiocarpal and midcarpal motion to the total amount of wrist motion. We defined *contribution ratio* as the percentage of the range of radiocarpal motion or midcarpal motion relative to the total amount of wrist motion. In this study, the contribution ratio was investigated only in the flexion-extension plane.

Statistical Analysis

All data were expressed as the mean with the standard deviation. Quantitative comparison of results between the control group and the RA group was performed using standard statistical formulas based on the Mann-Whitney U test. Results were deemed to be significant if $p < .05$.

RESULTS

Rheumatoid Arthritis Versus Normal

In the rheumatoid wrists, the average of total amount of wrist motion in the flexion-extension plane was 59° ± 20. The average range of radiocarpal motion in the flexion-extension plane was 27° ± 15 and that of midcarpal motion was 32° ± 17. In the normal wrists, the average of total amount of wrist motion in the flexion-extension plane was 111° ± 15. The average range of radiocarpal motion in the flexion-extension plane was 63° ± 14° and that of midcarpal motion was 47° ± 8. The ranges of radiocarpal motion ($p < .01$) and midcarpal motion ($p < .01$) in the flexion-extension plane in RA wrists were significantly less than normal as expected (Table 2). The average contribution ratios of radiocarpal and midcarpal joint in the flexion-extension plane were 46% and 54%, respectively, in RA wrists and 57% and 43%, respectively, in normal wrists (Fig. 3). On average, the midcarpal joint tended to have a greater contribution in the flexion-extension plane in RA wrists compared with normal wrists, even though the difference was not significant ($p = .179$).

Regarding the out of the plane motion of the wrists, the average of total amount of out of the plane motion (P/S) in RA was 8° ± 11 in supination during flexion motion of the wrist. The average range of out of the plane motion (P/S) in the radiocarpal joint was 5° ± 7 and that in the midcarpal joint was 2° ± 8 in supination during flexion motion of the wrists. In the normal wrists, the average of total amount of out of the plane motion (P/S) was 8° ± 13 in pronation during flexion motion of the wrists. The average range of out of the plane motion (P/S) in the radiocarpal joint was 3° ± 6 and that in the midcarpal joint was 4° ± 9 in pronation during flexion motion of the wrists. Consequently, during flexion motion of the wrists, the radiocarpal joint ($p < .01$) and the whole wrist joint, that is, the total for the radiocarpal and midcarpal joints ($p < .01$), significantly supinated in RA wrists compared with normal (Table 2).

The average of total amount of out of the plane motion (RD/UD) in RA was 5° ± 8 in ulnar deviation during flexion motion of the wrists. The average of out of the plane motion (RD/UD) in the radiocarpal joint was 1° ± 7 and that in the midcarpal joint was 4° ± 8 in ulnar deviation during flexion motion of the wrists. In the normal wrists, the average of total amount of out of the plane motion (RD/UD) was 8° ± 13 in radial deviation during flexion motion of the wrists. The average range of out of the plane motion (RD/UD) in the radiocarpal joint was 4° ± 8 and that in the midcarpal joint was 4° ± 8 in radial deviation during flexion motion of the wrists. Consequently, during flexion motion of the wrists, the midcarpal joint ($p < .05$) and the whole wrist joint, that is, the total for the radiocarpal and midcarpal joints ($p < .01$), significantly deviated ulnarly in RA wrists compared with normal (Table 2).

Stable Form Versus Unstable Form of RA

We classified the 30 rheumatoid wrists into 19 cases of stable form of disease and 11 cases of unstable form. The average of total ulnar translocation after onset of RA was 4.1 mm in the stable form and 10.7 mm in the unstable form; these values are consistent with the radiographic parameters described by Simmen and Huber (Table 1).[1] The average of total loss of carpal height ratio after onset of RA was 0.12 in the stable form and 0.28 in the unstable form; these values are also consistent with the radiographic parameters described by Simmen and Huber (Table 1).[1] Among the 11 wrists in the unstable form of disease, 7 showed S-L dissociation. In contrast, S-L dissociation was not found among the 19 wrists in the stable form of disease.

The range of radiocarpal and midcarpal motions in the flexion-extension plane varied greatly among cases in the stable form of disease (Fig. 4). In contrast, the range in cases of the unstable form was relatively constant; in 8 of the 11 wrists in unstable form, the midcarpal motion in the flexion-extension plane was greater than radiocarpal motion (Figs. 4, 5). Only 3 cases of the unstable form had greater motion in the radiocarpal joint than in the midcarpal joint (Fig. 4). The average ranges of radiocarpal and midcarpal motion in the flexion-extension plane were 31° ± 16 and 28° ± 15, respectively, in the stable form, and 20° ± 12 and 38° ± 19, respectively, in the unstable form. In the radiocarpal joint, the range of motion of the unstable form in the flexion-extension plane was significantly less than that of the stable form ($p < .05$), whereas in the midcarpal joint, there was no significant difference ($p < .05$) between the 2 groups (Table 3). The average contribution ratios of radiocarpal and midcarpal joint in the flexion-extension plane were 53% and 47%, respectively, in the stable form and 33% and 67%, respectively, in the unstable form (Fig. 6). In the midcarpal joint, the contribution ratio of the unstable-form group in the flexion-extension plane was significantly greater than that of the stable-form group ($p < .05$).

Regarding out of the plane motion (P/S) of the rheumatoid wrists, during flexion motion of the wrists, the